ARCHIVES OF ELECTRICAL ENGINEERING VOL. 61(4), pp. 443-454 (2012)

DOI 10.2478/v10171-012-0038-7

Comparative analysis of the chosen field-weakening methods for the Direct Rotor Flux Oriented Control drive system

K. NGUYEN-THAC, T. ORLOWSKA-KOWALSKA, G. TARCHALA[1]

Institute of Electrical Machines, Drives and Measurements
Wroclaw University of Technology
Smoluchowskiego 19, 50-372 Wroclaw, Poland
e-mail: {khanh.nguyen.thac/grzegorz.tarchala/teresa.orlowska-kowalska}@pwr.wroc.pl

(Received: 19.11.2011, revised: 26.04.2012)

Abstract: In this paper, an analysis of the induction motor control scheme based on the Direct Rotor Flux Oriented Control (DRFOC) for a whole speed range, including field-weakening (FW) regions is presented. Two field-weakening algorithms have been compared and verified through simulation with a 3.0 [kW] induction motor drive.

Key words: induction motor, optimal field-weakening, DRFOC

1. Introduction

In the field of closed loop controlled voltage source inverter fed induction motor (IM) drives the vector method based on the rotor flux oriented control (RFOC) with direct or indirect current control is the most used scheme, which it can be regarded as state of the art for various applications [1, 2]. In many applications, electrical drives have to deliver constant torque (rate or maximum) at low speed and to operate at almost constant power at medium and high speeds, where torque is decreased. In these cases, weakening of the motor flux is a suitable control method which results in and economic rating of the power converter and motor.

The most frequently applied method of field weakening (FW) control adjusts the excitation level of the machine by feed-forward control in inverse proportion to the mechanical speed of the motor. However, the 1990s showed renewed interest in the optimal methods for FW control of induction motors [3-7]. For rotor-flux orientation it was shown that the classical FW method of selecting the flux-producing current component proportional to the rotor speed inverse yields too large value, and a maximum torque is not achieved [4, 6, 7]. Various strategies for improved FW operation were proposed [8, 9]. The algorithm presented in [9] (a related scheme was proposed in [8]) for achieving the maximum torque is rather complex, because the control of the motor flux is obtained indirectly by controlling the motor current, and it require

the tuning of five PI regulators (two PI regulators are used for the current regulation, two PI regulators for the FW and another one for the speed regulation).

In the 2000s, several refinement techniques to improve or extend the last study results have been proposed. However, there exist some disadvantages, typically using several coefficients in [10] or to use multiple look-up table and complex formulas [11].

In this paper an optimal direct rotor flux oriented control (DRFOC) scheme to control IM in the whole speed range, including FW region, while maintaining stability and maximizing the torque production is analyzed. The performance of the DRFOC structure under such control is compared to that obtained using the classical $1/\omega_m$ control.

This paper is structured as follows. The current and voltage limits are discussed in Section 2. Then, the proposed algorithm is presented in Section 3; the control systems are shown in Section 4; followed by simulation results in Section 5. All simulation research are done for mathematical model of the IM written in per-unit system (according to [1, 2]). Conclusions are given in Section 6.

2. Current and voltage limits

The operating speed range of the IM drive can divide in three sub-regions: constant torque region ($\omega_s < \omega_{sb}$), constant power region ($\omega_{sb} \le \omega_s < \omega_{sc}$) and constant slip frequency region ($\omega_s \ge \omega_{sc}$) [1], as is shown in Figure 1 (where ω_{sb}, ω_{sc} are base and critical stator angular speeds).

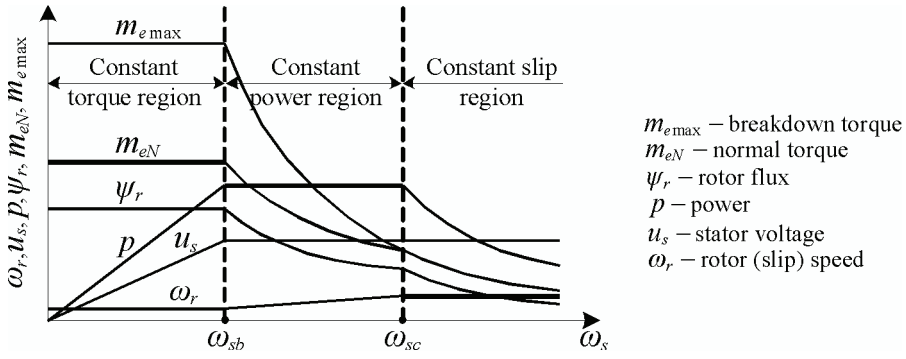

Fig. 1. Control characteristics of the induction motor in constant and weakened flux regions

The maximum torque of the induction motor is limited by the current and voltage ratings of the power inverter and thermal current limit of the IM. Therefore, it is useful to analyze performance of the machine under the current and voltage constraints in synchronous reference frame (x-y axes), rotating with the angular frequency $\omega_s = \omega_{s\psi}$.

The current constraint of the inverter can be expressed as follows:

$$i_{sx}^2 + i_{sy}^2 \le I_{\max}^2 , \tag{1}$$

where:

$$I_{\max} = |\mathbf{i}_s| = \sqrt{i_{sx}^2 + i_{sy}^2}$$

is the maximum stator current magnitude, and i_{sx}, i_{sy} are stator current vector components of the IM in the field-oriented $x - y$ coordinate system (rotating synchronously with the rotor flux angular frequency (ω_s). This relationship limits the current magnitude to the circle defined by $I_{\max}$.

The voltage constraint of the inverter is given as:

$$u_{sx}^2 + u_{sy}^2 \le U_{\max}^2 , \tag{2}$$

where u_{sx}, u_{sy} and U_{max} are the components of the stator voltage vector in $x - y$ coordinates and the maximum voltage magnitude, respectively.

U_{max} is set by the available voltage, which is function of the pulse-width-modulation strategy and the available DC-bus voltage (U_{dc}). This equation indicates that the voltage magnitude

$$|\mathbf{u}_s| = \sqrt{u_{sx}^2 + u_{sy}^2}$$

cannot exceed the ellipse defined by U_{max} [5]. Nowadays mainly the Space Vector Modulation (SVPWM) is used, thus the U_{max} is limited in the linear region to $U_{dc}/\sqrt{3}$, however, overmodulation can allow $2U_{dc}/\pi$.

The steady-state stator voltage equations of the IM are given directly from the motor mathematical model [2]:

$$u_{sx} = r_s i_{sx} - \omega_s \sigma x_s i_{sy} , \tag{3}$$

$$u_{sy} = r_s i_{sy} + \omega_s x_s i_{sx} , \tag{4}$$

where r_r, r_s – rotor and stator winding resistance, x_r, x_s – rotor and stator winding self-inductance, x_M – induction motor main inductance, $\sigma = 1 - x_M^2 / x_r x_s$ – total leakage factor. It should be mentioned that in [p.u.] the values of inductance and reactance are the same [1, 2].

The equation for the voltage limit ellipse (5) and current limit ellipse (6) can be derived by substituting (3), (4) into (2) and (1):

$$\left(\frac{r_s i_{sy}}{U_{\max}} + \frac{x_s i_{sx}}{U_{\max}/\omega_s}\right)^2 + \left(\frac{r_s i_{sx}}{U_{\max}} - \frac{\sigma x_s i_{sy}}{U_{\max}/\omega_s}\right)^2 \le 1, \tag{5}$$

$$\left(\frac{u_{sx} r_s + \omega_s \sigma x_s u_{sy}}{I_{\max}(r_s^2 + \omega_s^2 \sigma x_s^2)}\right)^2 + \left(\frac{u_{sy} r_s - \omega_s x_s u_{sx}}{I_{\max}(r_s^2 + \omega_s^2 \sigma x_s^2)}\right)^2 \le 1. \tag{6}$$

In the case of rotor flux oriented control of the IM, the rotor flux and torque can be described as follows [2]:

$$\boldsymbol{\psi} = \boldsymbol{\psi}_r = \boldsymbol{\psi}_{rx} = x_M i_{sx}, \tag{7}$$

$$m_e = \frac{x_M}{x_r}\psi_r i_{sy} = \frac{x_M^2}{x_r} i_{sx} i_{sy}. \tag{8}$$

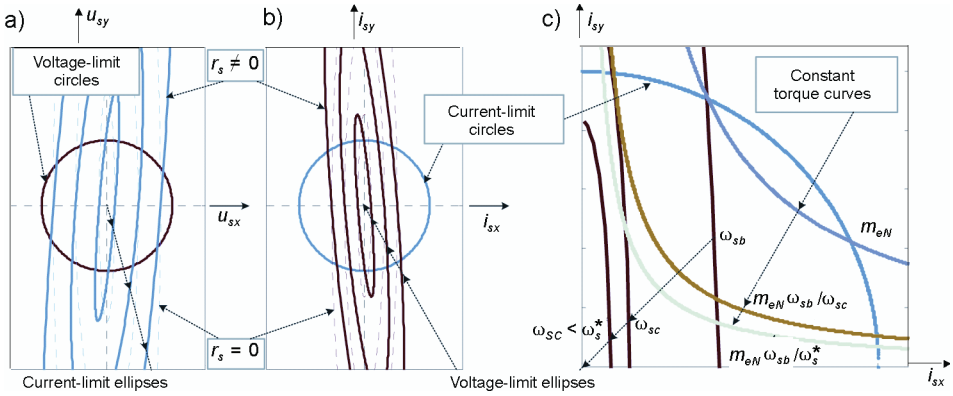

Fig. 2. a) Voltage-limit circle (2) and current-limit ellipse (6); b) current-limit circle (1) and voltage-limit ellipse (5); c) detailed of Figure 2b with data of investigated induction machine

Basing on those expressions, the current limit circle (with $I_{max} = 1$ [p.u.]), three voltage limit ellipses (with $U_{max} = 1$ [p.u.], $\omega_s = \omega_{sb}$, $\omega_s = \omega_{sc}$ and $\omega_s = \omega_s^* > \omega_{sc}$) and three constant torque curves (with $m_e = m_{eN}$, $m_e = m_{eN}\omega_{sb}/\omega_{sc}$, $m_e = m_{eN}\omega_{sb}/\omega_s^*$) are presented in Figure 2c. The dotted line ellipses in Figure 2a, b are form of the constraints when the stator resistance is neglected. In contrast, the bold line ellipses are the constraints when the stator resistance is included. The stator resistance is affecting the operating conditions of the IM at low speeds region (5) and can be neglected in high speed region. The centre of the voltage limit ellipse (Fig. 2b, c) is the origin, which implies that as the frequency increases or voltage decreases, the voltage constraint will shrink toward the origin (according to (5)).

3. Field weakening algorithms

The field weakening algorithm should provide robust and stable current regulation in whole range speed included FW region by making sure that the IM is operated within the voltage and the current maximum constraints. Under the assumption of the slow enough variation of the rotor flux and the precise vector control, the current maximizing the torque (8) of the IM, can be derived from the constraints given by (1), (2) and (5). The size of the ellipse by the voltage constraint (5) decreases as the operating speed increases as shown in Figure 2. The current constraint in (1) can be depicted as a circle in the current plane as shown in Figure 2. The possible operating region is the inside area of the current circle and voltage ellipse and the torque is depicted as a reciprocal proportion curve in the current plane as shown in Figure 2a.

A) Constant torque region ($\omega_s < \omega_{sb}$)

If the i_{sx} current for the maximum torque, which is the current at the crossing point of the ellipse and the circle, is larger than its rated value i_{sxN}, it should be set as the rated value i_{sx}^c to prevent the magnetic saturation of the IM. That is the case of point B_1 in Figure 3, where the torque m_{e1} may be obtained by i_{sx1} but larger than i_{sxN} and it would result in the severe saturation of the magnetic circuit of IM. In this case, i_{sx}^c should be set as i_{sxN} as (9):

$$i_{sx}^c = i_{sxN} = \psi_{rN} / x_M \tag{9}$$

and the operating point should be B in the Figure 3, generating torque m_{e2}.

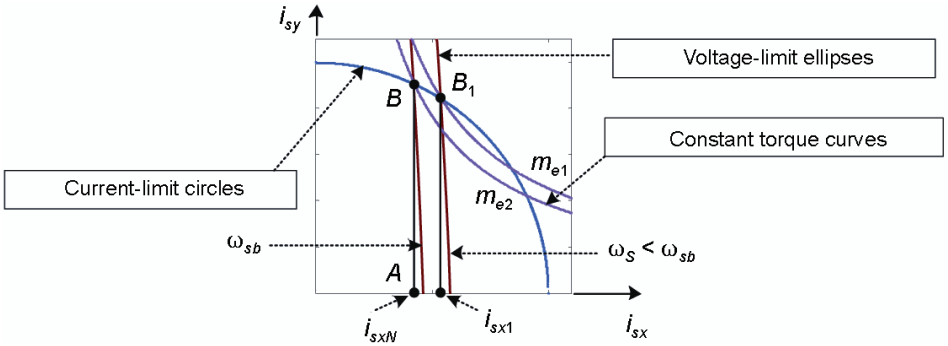

Fig. 3. Constant torque region

Also, the maximum available torque is decided only by the maximum i_{sy}^c current component, which is given by the current constraint (10):

$$i_{sy\,\mathrm{lim}}^c = \sqrt{I_{\max}^2 - i_{sxN}^2} \quad \text{or} \quad i_{sy}^c \le \sqrt{I_{\max}^2 - i_{sxN}^2} \tag{10}$$

and the maximum torque always the same as m_{e2} in this region; operation point of the motor should lie on line AB with constant i_{sx}^c. Hence, the region is called the constant torque region.

Thus the rotor flux reference value can be calculated as follows:

$$\psi_r^c = \psi_{rx}^c = x_M i_{sx}^c . \tag{11}$$

As the speed increases and the side of the ellipse decreases, the circle coincides with the nominal current, i_{sxN}. The angular frequency where the constant torque operation region ends is defined as the stator base frequency, ω_b and neglecting the stator resistance; it can be obtained from (5) as follows:

$$\omega_{sb} = \frac{U_{s\max}}{x_s \sqrt{i_{sxN}^2 (1-\sigma^2) + \sigma^2 I_{\max}^2}} . \tag{12}$$

Thus the base mechanical speed, ω_{mb}, of the motoring mode can be obtained:

$$\omega_{mb} = \omega_{sb} - \omega_{rN}, \tag{13}$$

where ω_{rN} is rated rotor (slip) angular frequency.

B) Constant power region ($\omega_{sb} \leq \omega_s < \omega_{sc}$) – field weakening region I

In this operation region of the IM, delivering the rated power, the torque production will be inversely proportionally to the speed:

$$m_e = \frac{x_M^2}{x_r} i_{sx} i_{sy} \sim \frac{1}{\omega_m} \cong \frac{1}{\omega_s}. \tag{14}$$

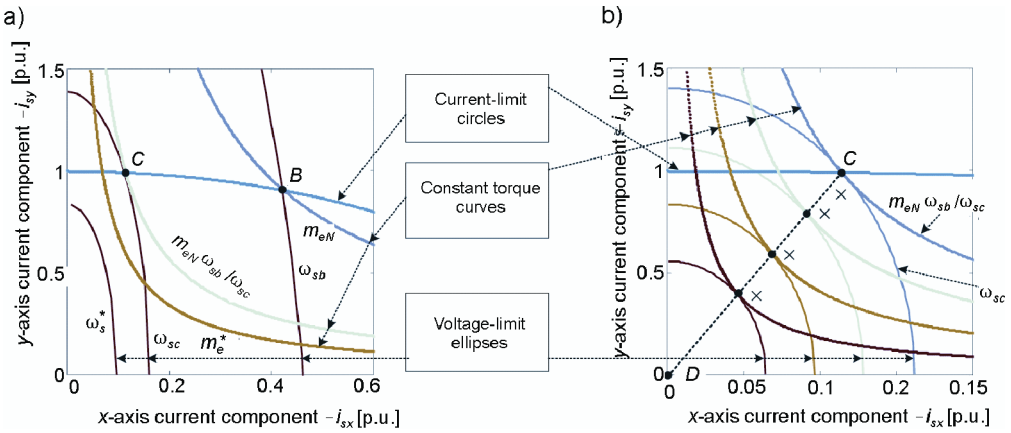

Fig. 4. Field weakening region I (a) and field weakening region II (b)

This operation region starts from the base speed, ω_{sb} (point B in Fig. 4a), and ends at a critical speed, ω_{sc} (point C in Fig. 4a), above which there is no more crossing point between the ellipse (at ω_s^c) and the constant torque curve (at command torque value $m_e^c = m_{eN}\omega_{sb}/\omega_s^c$) – for example an ellipse with ω_s^* and torque curve m_e^* in Figure 4a.

In Figure 4a, to obtain maximum torque in FW region I, the current vector must slide on line B-C, which is intersection between the current circle limit, the voltage ellipse limit and the constant torque curve. When $\omega_s = \omega_{sc}$, the voltage ellipse limit and the constant torque curve (at $m_e = m_{eN}\,\omega_{sb}/\omega_{sc}$) intersect each other at only one point (contact point C).

The command currents (i_{sx}^c, i_{sy}^c) for maximizing the motor torque can be obtained while Equation (5) and assumed stator resistance is neglected:

$$i_{sx}^c = \frac{\sqrt{U_{\max}^2 - \omega_e^2 x_s^2 \sigma^2 I_{\max}^2}}{\omega_e x_s \sqrt{1-\sigma^2}} \quad \text{and} \quad i_{sy\,\lim}^c = \sqrt{I_{\max}^2 - (i_{sx}^c)^2}. \tag{15}$$

Simultaneously the rotor command flux can be obtained as (11).

In this region, the slip angular frequency is increased as the speed increases. As the speed is further increased, the slip reaches the maximum value due to the voltage limit and then the II FW region begins. The slip speed value for maximum torque is given by the following expression [1]:

$$\omega_{r\max}\frac{r_r}{\sigma x_r}. \tag{16}$$

C) Constant slip region ($\omega_s \geq \omega_{sc}$) – field weakening region II

As the slip angular frequency and the speed are further increased, the stator operating frequency is further increased, and the ellipse is more reduced and its large portion begins to be included in the circle shown in Figure 4b.

The onset of region II ω_{sc} is time when for the optimal current values (points × in line C-D in the Figure 4b) for given maximum torque only the voltage limits is the constraint to be considered. The steady-state electrical torque is proportional to $i_{sx}i_{sy}$ (8). From (3) and (4), if r_s is neglected, we have $u_{sx} = -\omega_s\sigma x_s i_{sy}$ and $u_{sy} = \omega_s x_s i_{sx}$, it is found that when maximum voltage is applied, $\mathbf{u} = U_{\max}e^{j\varphi}$, $i_{sx}i_{sy}$ is proportional to $u_{sx}u_{sy} = 1/2U_{\max}^2\sin 2\varphi$. Thus, the torque is maximized if $\sin 2\varphi = 1$, i.e., $|u_{sx}| = |u_{sy}| = U_{\max}/\sqrt{2}$. Therefore, the optimal current components for the maximum torque can be obtained as (17) and rotor command flux as (11):

$$i_{sx}^c = \frac{U_{\max}^2}{\sqrt{2\sigma x_s I_{\max}^2}} \text{ and } i_{sy\lim}^c = \frac{U_{\max}}{\sqrt{2}\omega_s\sigma x_s}. \tag{17}$$

Assumed that stator resistance is neglected, substituting (17) into (1) we obtain ω_{sc} as (18):

$$\omega_{sc} = \frac{U_{\max}\sqrt{2(\sigma^2+1)}}{2\sigma x_s I_{\max}}. \tag{18}$$

Figure 4b shows the trajectory (dash line) of this optimal current vector. In this region, i_{sy}^c should be decreased with the reduction of i_{sx}^c in order to keep the maximum slip.

D) Influence of the stator resistance on the FW algorithm

When stator resistance (r_s) is taken into account, the value of the reference flux current i_{sx}^c is reduced (i.e. ψ_r^c is reduced). In Figure 5 the influence of the r_s and also U_{max} on the flux current component in the FW regions presented. In the Figure 5, lines (a), (b), (c), and (d) are presented respectively: the flux current i_{sx}^c without r_s, i_{sx}^c with r_s, absolute difference and relative difference between two cases of flux current respectively. However, when U_{max} is reduced, the differences increase especially in the FW region II.

The detailed sensitivity analysis of the FW algorithm to the motor parameter changes will be published in the other paper, which is now prepared.

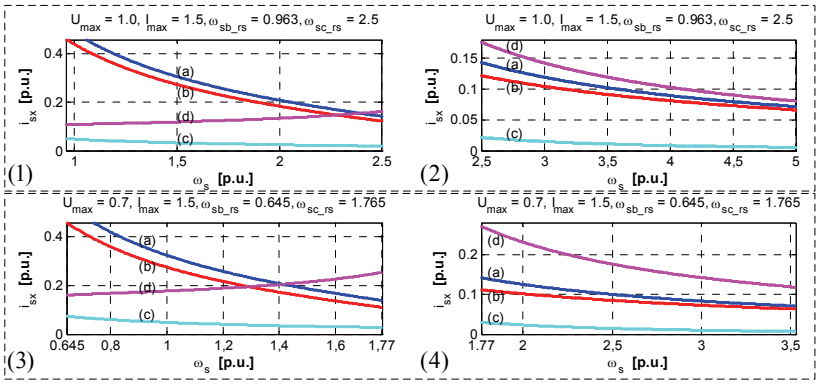

Fig. 5. Influence of the stator resistance on the flux current component in FW region for I_{max} = 1.5 [p.u.] and: (1) FW region I and (2) FW region II with U_{max} = 1.0 [p.u.]; (3) FW region I and (4) FW region II with U_{max} = 0.7 [p.u.]

E) The classical method ("$1/\omega_m$" method)

For the FW operation, a commonly used method is to vary the rotor flux reference inversely proportional to the rotor speed ω_m. In this method, the command currents i_{sx}^c and i_{sy}^c in the FW region are given as

$$i_{sx}^c = \frac{\omega_{mb}}{\omega_m} i_{sxN}\,, \tag{19}$$

$$i_{sy\,\mathrm{lim}}^c = \sqrt{I_{\max}^2 - (i_{sx}^c)^2} \quad \text{or} \quad i_{sy}^c \le \sqrt{I_{\max}^2 - (i_{sx}^c)^2}\,. \tag{20}$$

Combine (19) and (20) we obtain the limit constraint of this method as:

$$\left(i_{sy}^c\right)^2 + \left(i_{sxN}\omega_{mb}/\omega_m\right)^2 = I_{\max}^2. \tag{21}$$

Equation (21) describes that when the rotor flux is reduced according to $1/\omega_m$, the trajectory of the reference current vector $\mathbf{i}_s^c = i_{sx}^c + j i_{sy}^c$ moves along the current limit circle as the speed increase. Therefore, the voltage limit is not considered in this method. As a result, the voltage margin enough to regulate the current reference cannot be maintained. Thus, in a high speed region (FW region I) the IM operating may be unstable depending on the machine parameters. In a very high speed region (FW region II), this method does not guarantee the condition (17), the drive system is operated in an unstable torque region. As a result, the current control falls and the drive system losses its controllability.

4. Control systems implementation

The analysed classical DRFOC scheme for the IM drive system is shown in Figure 6. The structure consists of two independent control loops, one – for the rotor flux control and the second – for electromagnetic torque and speed control [2].

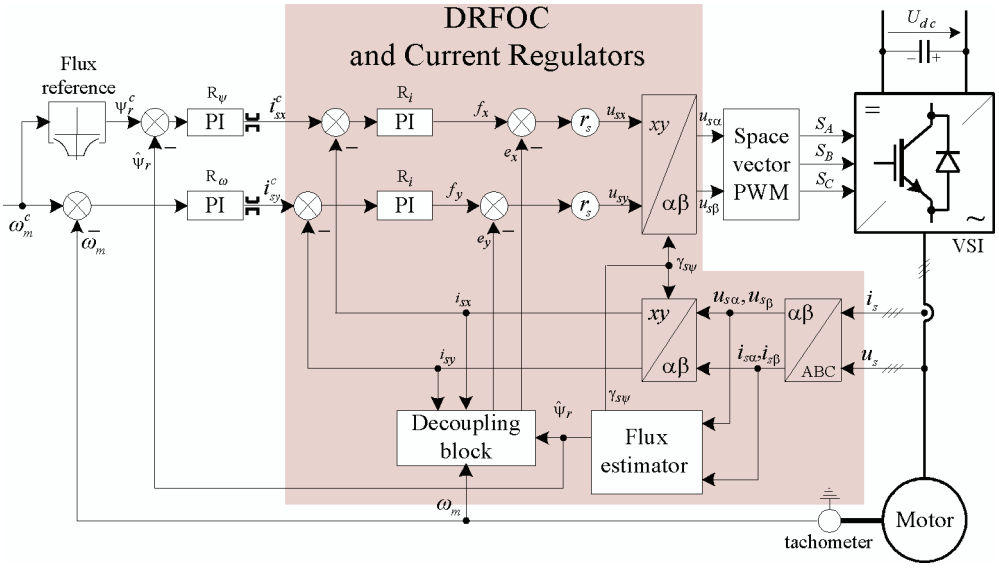

Fig. 6. Block diagram of the classical scheme

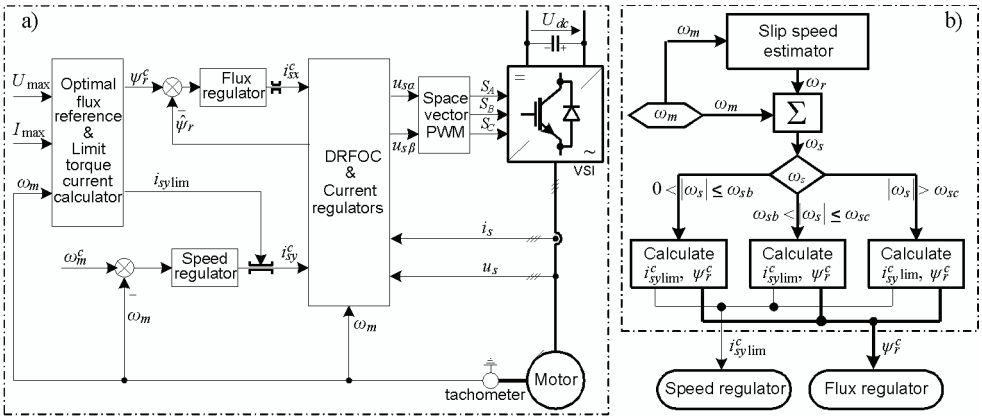

Fig. 7. Block diagram of the proposed control structure (a) and the optimal flux reference algorithm scheme (b)

These control loops consist of the supervised rotor flux regulator and the current component i_{sx} regulator (which is responsible for the rotor flux control) as well as the independent speed regulator and the current component i_{sy} regulator (which is responsible for the motor torque control). The rotor flux command is determined with $1/\omega_m$ method in the classical structure. The control structure is equipped also with the rotor flux estimator and decoupling block which perform the linearization of the stator winding mathematical model to obtain the independent rotor flux and electromagnetic torque regulation using stator current components in the field-oriented reference frame (x – y).

In Figure 7a the classical flux command is replaced with more advanced optimal field-weakening algorithm, described in the previous section, which is shown in the block diagram of Figure 7b.

5. Simulation results

In the following figures chose simulation results for tests of both flux weakening algorithms are presented and compared (with $P_N = 3.0$ [kW], $n_N = 1400$ [rpm], and following per-unit parameters of the equivalent circuit: $r_s = 0.0707$, $r_r = 0.0637$, $x_s = x_r = 1.9761$, $x_M = 1.8780$). Simulations were performed for the same voltage and current limit constraints ($I_{max} = 1.5$ [p.u.], $U_{max} = 1.0$ [p.u.]), thus we obtained the value of the base and critical speeds as $\omega_{sb} = 0.963$ [p.u.], $\omega_{sc} = 2.5$ [p.u.]. For each test, two schemes used the same character of load torque. Test results for the classical scheme are demonstrated in the left hand side of each figure, and for the optimal FW algorithm – in the right hand side, respectively.

In Figure 8 simulation results under start up (with linear speed reference ramp), steady state at 1.8 [p.u.] speed, maximal load torque $m_L = 0.35$ [p.u.] and braking cycle in both directions are shown. In this speed range, the operation results of two schemes are quite similar and no differences in all state variables are observed.

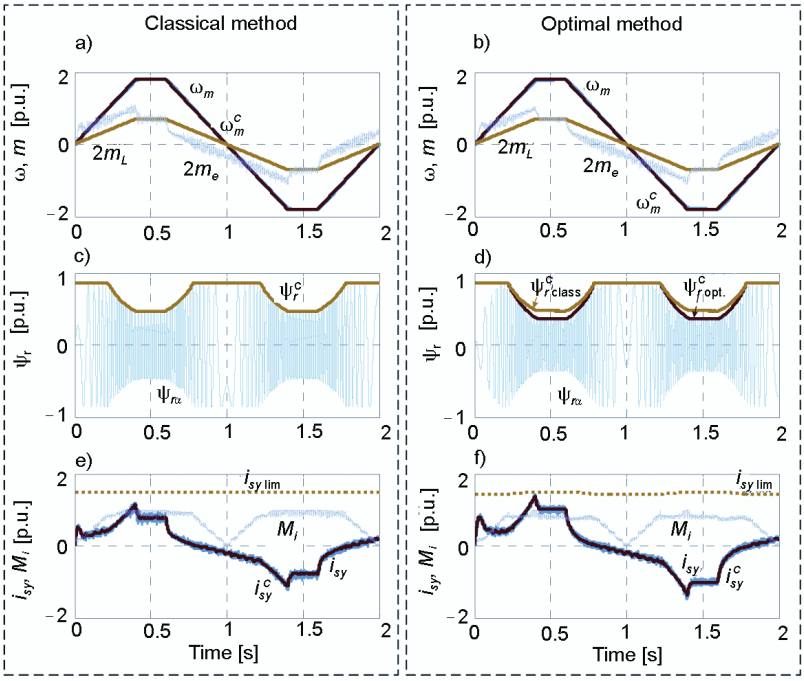

Fig. 8. Start up, steady state at 1.8 [p.u.] speed and braking cycle in both direction: (a, b) reference and motor speeds, load and motor torques, (c, d) rotor flux, (e, f) modulation index and stator current torque components

In Figure 9 the similar results are shown, but for the maximal steady-state reference speed at 2.6 [p.u.] and maximal allowable load torque $m_L = 0.24$ [p.u.]. In these operation condition, we obtained a lot of differences between the two control algorithms.

First, an unstable torque current i_{sy} operation appears, when the load torque changes at high speed in the classical scheme (Fig. 9a). That is clear, as the scheme does not guarantee the stability due to the limited voltage conditions, what we can see at the Figure 9c. When the process of braking begins, the operation point runs on the current-limit circle, and thus the stator current component i_{sy} decreases and i_{sx} increases simultaneously. But the current i_{sx} cannot be larger than i_{sxN}, therefore i_{sy} becomes discontinuous at i_{sxN}, it jumps from i_{sy} to $-i_{sy}$ and fast runs towards to the value $-I_{max}$. As a result of (1), the $i_{sx} \approx 0$ and $\psi_r \approx 0$.

Next, in the high speed region, the reference flux of the optimal scheme at a steady state (e.g. $t = 0.6$s) is smaller than in the classical scheme (0.23 versus 0.33, see Fig. 9d), which guarantees that torque current component will be larger (compare Fig. 9e, f), so it can give the fast response of the torque and speed (see Fig. 9a, b).

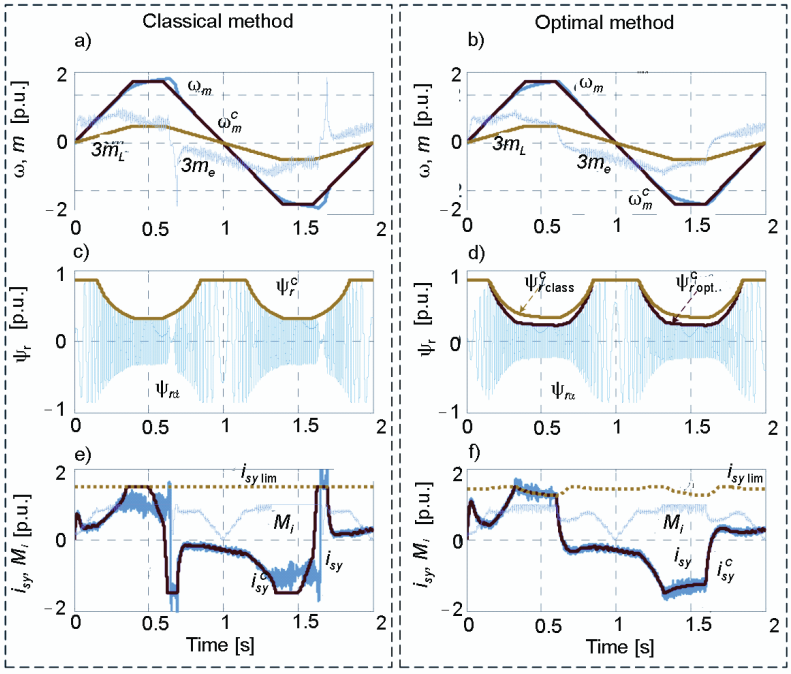

Fig. 9. Start up, steady state at 2. 6 [p.u.] speed and braking cycle in both directions: (a, b) reference and motor speeds, load and motor torques, (c, d) rotor flux, (e, f) modulation index and stator current torque components

6. Conclusion

For the field weakened operation of the induction motor drives a commonly used method is to vary the rotor flux reference in proportion to $1/\omega_m$. However in this method, because only

the current limit is considered, the system cannot produce maximum torque, and is unstable in the high speed region.

In the contrary, the algorithm for FW with maintaining the voltage and current limits, guarantee the stable operation of the IM drive in the whole speed range. The algorithm presented in this paper enables to calculate the optimal flux reference for the DRFOC structure and to limit the torque current set value. This scheme to maintain the maximum torque capability of an IM over whole speed range included FW region is especially dedicated to drives operating in the wide speed region, as traction drives. In this scheme the base speed, maximum slip frequency and transition speed between two sub-regions of the FW, depending on the condition of the voltage and current limits, is automatically calculated, so smooth transition between speed regions is obtained.

The proposed scheme is compared with the classical method through simulations. And it is verified that the new scheme provides the improved torque capability over the classical FW one.

In the nearest future authors would like to verify the proposed algorithm in the laboratory set-up.

Acknowledgements

This research work was supported partly by the Ministry of Science and Higher Education, Poland, under Grant N R01 0001 06/2009 (2009-2012).

References

[1] Kaźmierkowski M.P., Tunia H., *Automatic control of converter-fed drives*. Elsevier (1994).
[2] Orłowska-Kowalska T., *Sensorless induction motor drives.* Wroclaw University of Technology Press, Wroclaw, Poland (2003) (in Polish).
[3] Xu X., De Doncker R., Novotny D.W., *Stator flux orientation control of induction machines in the field weakening region.* IEEE Industry Appl. Soc. Ann. Meeting 431: 437-443 (1988).
[4] Xu X.Y., Novotny D.W., *Selection of the Flux Reference for Induction Machine Drives in the Field Weakening Region.* IEEE Trans. Ind. Appl. 28(6): 1353-1358 (1992).
[5] Novotny D.W., Lipo T.A., *Vector Control and Dynamics of Ac Drives*. Clarendon Press (1996).
[6] Grotstollen H., Bunte A., *Control of induction motor with orientation on rotor flux or on stator flux in a very wide field weakening region – Experimental results.* ISIE'96 – Proc. of the IEEE Int. Symp. on Industrial Electronics 1, 2: 911-916 (1996).
[7] Kim S.H., Sul S.K., *Maximum Torque Control of an Induction Machine in the Field Weakening Region.* IEEE Trans. Ind. Appl. 31(4): 787-794 (1995).
[8] Grotstollen H., Wiesing J., *Torque Capability and Control of a Saturated Induction-Motor over a Wide-Range of Flux Weakening.* IEEE Trans. Ind. Electron. 42(4): 374-381 (1995).
[9] Kim S.H., Sul S.K., *Voltage control strategy for maximum torque operation of an induction machine in the field-weakening region.* IEEE Trans. Ind. Electron. 44(4): 512-518 (1997).
[10] Harnefors L., Pietilainen K., Gertmar L., *Torque-maximizing field-weakening control: Design, analysis, and parameter selection.* IEEE Trans. Ind. Electron. 48(1): 161-168 (2001).
[11] Gallegos-Lopez G., Gunawan F.S., Walters J.E., *Current control of induction machines in the field-weakened region.* IEEE Trans. Ind. Appl. 43(4): 981-989 (2007).